Supporting Information for

Beyond Stretchability: Strength, Toughness, and Elastic Range in Semiconducting Polymers

Alexander X. Chen, Andrew T. Kleinschmidt, Kartik Choudhary, and Darren J. Lipomi*

Department of NanoEngineering and Program in Chemical Engineering, University of California, San Diego, 9500 Gilman Dr. Mail Code 0448, La Jolla, CA, 92093-0448

*Correspondence to: dlipomi@eng.ucsd.edu

1. Supporting Information

1.1 Effect of Sample Thickness and Strain Rate

The mechanical properties of a semiconducting film are not just dependent on the material itself, but also the physical characteristics of the sample (e.g. thickness, geometry) and the testing parameters (external factors e.g. temperature, strain rate, pressure, humidity). Device design and optimization therefore requires a thorough understanding of how the physical characteristics and external factors affect the mechanical properties. For example, a flexible wearable device must be able to handle a wide range of strain rates. The same is true for other external factors (e.g. humidity, temperature, pressure, etc.). **Figure S1** and **Figure S2** show how the mechanical properties of poly(3-hexylthiophene) (P3HT) and diketopyrrolopyrrole (DPP)–based polymer films change relative to increasing strain rate (**Figure S1**) and increasing thickness (**Figure S2**).

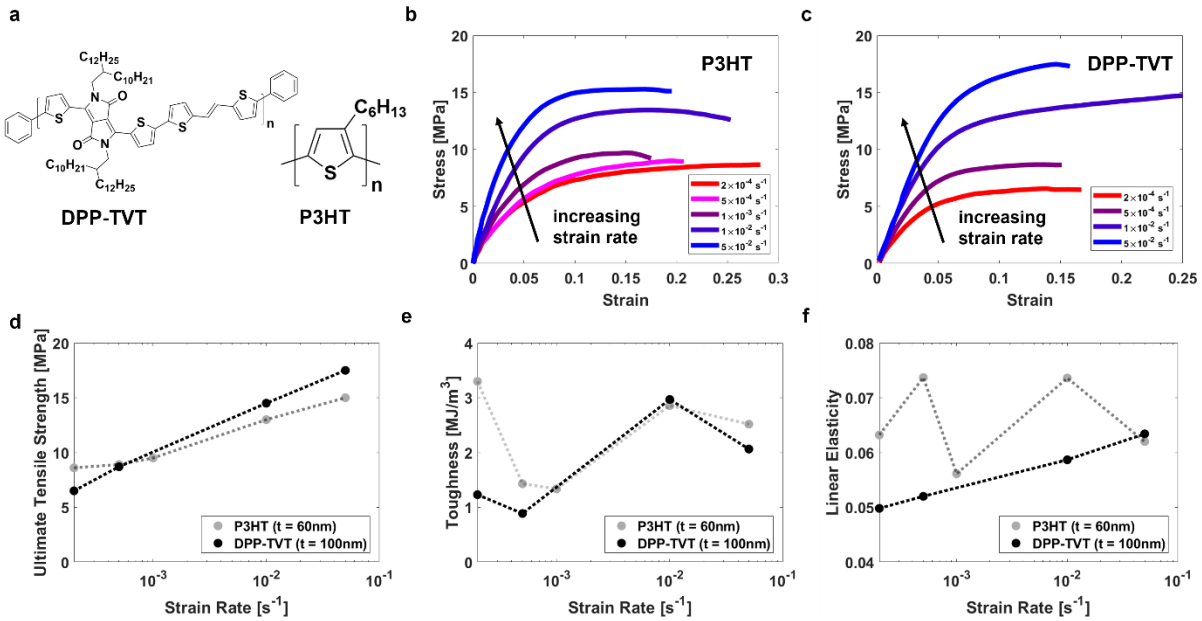

Figure S1. Mechanical properties of P3HT (60 nm) and DPP-TVT (100nm) as a function of tensile-testing strain rate. (a) Chemical structures of P3HT and DPP-TVT. (b) Stress-strain curves of P3HT and (c) DPP-TVT films as a function of strain rate as replotted from Zhang et al. 2018.[1] (d) Tensile strength increased as a function of strain rate. (e) Toughness remained relatively constant as a function of strain rate. (f) The range of linear elasticity increased relative to strain rate for P3HT and remained relatively constant relative to strain rate for DPP-TVT.

Conjugated polymers, much like their nonconjugated counterparts, exhibit rate dependent mechanical behavior.[2] Both P3HT and DPP-TVT are semicrystalline polymers that have glass transition temperatures below room temperature.[1,3] Their low T_g make it so that they exhibit viscoelastic behavior at T > T_g. Higher strain rates give polymer chains less time to arrange themselves in more favorable configurations, thus reducing their conformational degrees of freedom.[1,2] This results in a higher measurement of tensile strength (**Fig S1d**) and related properties (e.g. yield stress) due to the increased resistance to deformation.[1] At lower strain rates, polymer chains are able to dissipate energy by stretching and shifting to more favorable equilibrium positions.[2] For this reason, lower strain rates generally result in a higher fracture strain. An analogous example would be stretching a plastic bag; pulling both sides of the bag quickly

results in instantaneous failure of covalent bonds and forcing chain pullout,[4] thus forming a hole immediately. However, pulling the bag slowly results in the plastic getting thinner and thinner as it stretches, until it eventually tears apart at the weakest (thinnest) point. In these samples, we see that the tensile strength increases as the strain rate increases as expected. However, Zhang et al. noted that the fracture strain is greatly affected by the presence of intrinsic defects in the film, and thus causes deviations in expected behavior.

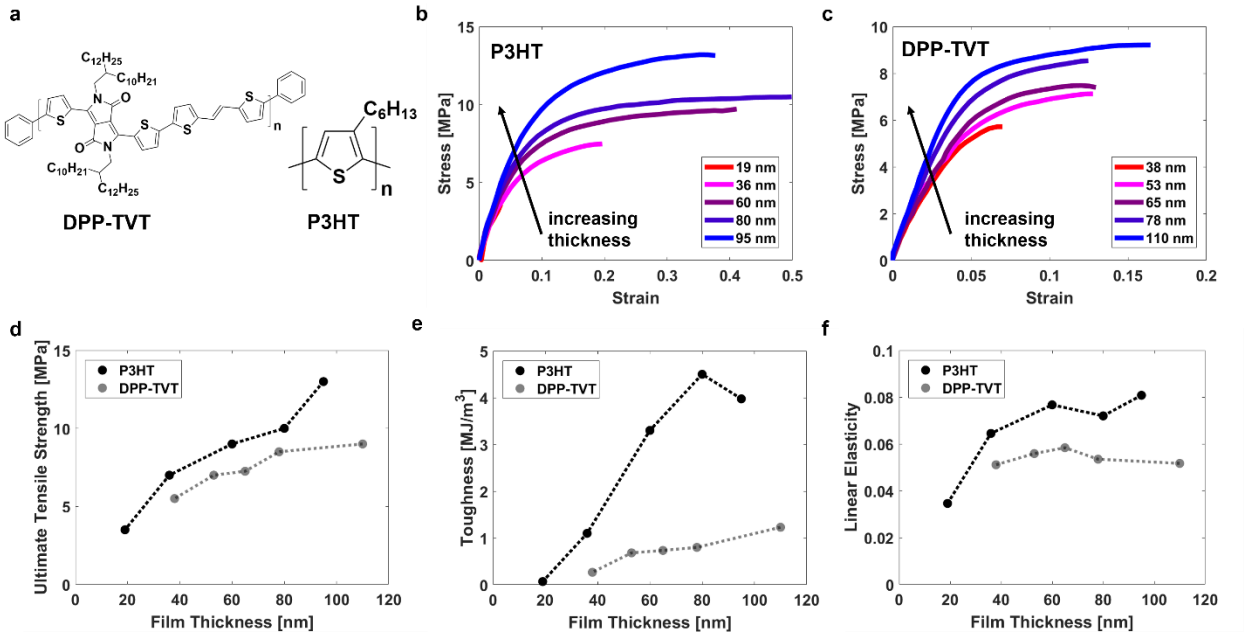

Figure S2. Mechanical properties of P3HT and DPP-TVT as a function of film thickness. (a) Chemical structures of P3HT and DPP-TVT. (b) Stress-strain curves of P3HT and (c) DPP-TVT films as a function of thickness as replotted from Zhang et al. 2018.[1] (d) Tensile strength and (e) toughness increased relative to increasing film thickness for both P3HT and DPP-TVT. (f) The range of linear elasticity increased relative to thickness for DPP-TVT and remained relatively constant relative to thickness for P3HT.

Both P3HT and DPP-TVT show an increase in tensile strength (**Fig S2d**) and fracture strain relative to increasing film thickness. Thus, increasing the thickness of the film consequentially results in an increase in the toughness (**Fig S2e**). The mechanical properties of thin conjugated

polymer films are highly dependent on thickness for three main reasons: (1) skin-depth effects (by this, we mean differences between surface and bulk morphology), (2) chain confinement effects, and (3) surface roughness. Due to skin-depth effects, extremely thin films have highly mobile polymer chains and fewer entanglements when the entire sample is "near the surface".[5] As a result, the intermolecular forces between chains are weakened, softening the material. This microstructure additionally results in a lower T_g as well as a lower modulus and fracture strength.[5] The morphology of the film is also affected by the confinement of the polymer chains between the substrate and the free interface.[6] By this, we mean that the coil conformations and arrangement of the polymer chains become more perturbed as the thickness decreases.[6] Finally, the surface roughness is also a significant consideration for thin films due to its effect on the geometry of the sample. Previous work by Rodriquez et al. has shown that P3HT films with thicknesses between 100 nm – 200 nm can have a peak-to-valley roughness of 25–35 nm.[7] Significant disparities in film thickness can lead to stress concentrating in the thinnest regions of the film, resulting in premature fracture and lower tensile strengths. Likewise, the effect of intrinsic material defects is exacerbated for thinner films with rougher surfaces. In an ideal film, a decreasing thickness generally corresponds to a slight increase in fracture strain due to the increased mobility of the polymer chains.[5] However, this is the opposite of what we see in **Fig S2b-c**. We can attribute this mismatch between theory and data to nonideal testing due to (1) rougher (relatively speaking) surfaces for thinner films, (2) stress concentration in thinner regions or film defects.

1.2 Effect of Solvent

The thermodynamics of polymer solutions has been extensively studied (e.g. Flory–Huggins solution theory,[8–10] Mark–Houwink equation,[11,12] intermolecular forces,[13] kinetic

behavior, etc.). It is well known that the structure, conformation, and physical properties of a polymer film are in part dependent on the properties of the solvent.[14] A "good" solvent refers to a polymer-solvent mixture in which interactions between polymer chains and solvent molecules are more energetically favorable, promoting high solubility. This is in contrast to a "poor" solvent, in which polymer-polymer interactions are more energetically favorable, promoting aggregation of polymer chains. In the last few decades, many papers have been dedicated to elucidating how the solvent affects morphology after deposition, and how this in turn affects electronic (and to a lesser extent, mechanical)[15,16] properties.[17–22] **Figure S3** below shows how the mechanical properties of interest for a donor–acceptor (D–A) polymer film change relative to the dielectric constant of the solvent.

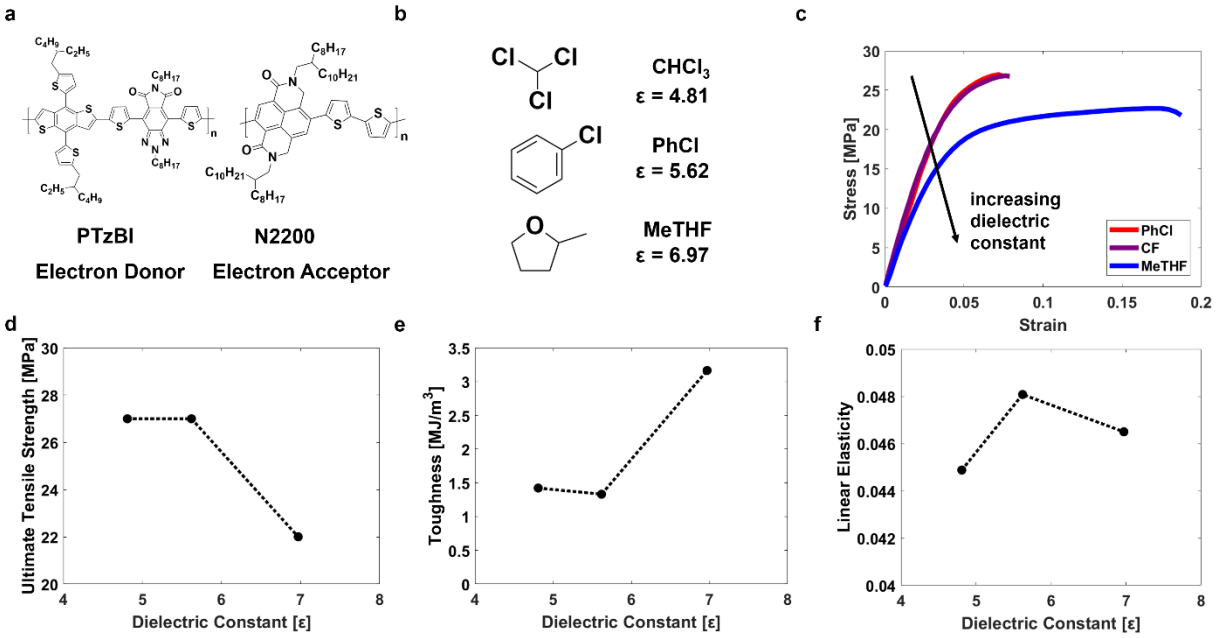

Figure S3. Mechanical properties of PTzBI:N2200 thin films relative to the dielectric constant of the solvent. (a) Chemical structures of PTzBI (donor polymer) and N2200 (acceptor polymer). (b) The solvents used for the polymer solutions are as follows from top to bottom: chloroform (CF), chlorobenzene (PhCl), and 2-methyltetrahydrofuran (MeTHF). (c) Stress-strain curves of PTzBI:N2200 polymer films as replotted from Lin et al. 2019.[16] (d) Tensile strength, (e) toughness, and (f) linear elasticity are shown relative to dielectric constant of the solvent.

For the sake of simplicity, we summarize all property changes associated with varying the solvent (e.g. boiling point, polarity, solubility) as the change in one predominant, systematic variable: the dielectric constant (ε) of the solvent. The dielectric constant is a general measurement of the polarizability (increasing ε corresponds to increasing polarizability) of the solvent, and thus greatly affects the properties and solvent "quality" of the polymer solution. CF and PhCl have relatively similar dielectric constants, and thus similar mechanical properties. In general, a decrease in solvent polarity correlated with a decrease in tensile strength (**Fig S3d**) and increase in toughness (**Fig S3e**). The increase in toughness is largely due to the increased fracture strain for the MeTHF sample. The range of linear elasticity remained approximately constant (**Fig S3f**).

UV-vis absorption spectra showed stronger aggregation of N2200 in MeTHF than in CF and PhCl, which suggests that MeTHF is a poorer solvent. Additional GIWAXS data suggests that the CF and PhCl films induce strong crystallization and highly ordered films, while the MeTHF indicates weak crystallization and disorder. The authors suggested that this was due to (1) the blade coating deposition process reducing solubility due to the temperature gradient between the high temperature solution and low temperature substrate[16] and (2) MeTHF evaporating faster (due to its lower boiling point), both of which suppress crystalline growth. As a poorer solvent, MeTHF induces a morphological structure more favorable for increasing the extensibility of a film. The opposite is true as well: better solvents like CF and PhCl induce a more favorable morphology for increasing the tensile strength.

The majority of the samples discussed in this Perspective were deposited by spin coating films onto a substrate.[23] These samples, however, were deposited using a blade coating technique. Shearing deposition techniques (e.g. blade coating) induce anisotropy in thin films by promoting

chain alignment,[24] and thus the mechanical (and electronic) properties of a blade coated film differ from those of a spun film. Despite this, there have been few if any studies (to the best of our knowledge) comparing how different deposition techniques affect the mechanical properties of semiconducting polymer films.

1.3 Effect of P3HT Nanowire Composition

Nanowires (NWs) are useful structures for many semiconducting polymer applications (e.g. chemical and biological sensing, electrical interconnects, transistors) due to their unique electronic properties and geometry.[25] Their high ratio of area to volume allows for greater surface area for diffusion, adsorption/desorption, and electrical response.[25] However, NWs also offer an opportunity to achieve favorable morphologies for different device applications by altering the microstructure of a polymer film. For example, conjugated polymer nanowires have been used to achieve percolated networks in polymer matrices that are both mechanically stable and improve electronic performance.[26,27] Likewise, semiconducting polymer NWs have been shown to conduct charge even in an insulating polymer matrix.[28] Shown below in **Figure S4** is a comparison of P3HT films blended with varying fractions of P3HT NWs as conducted by Kim et al.[27]

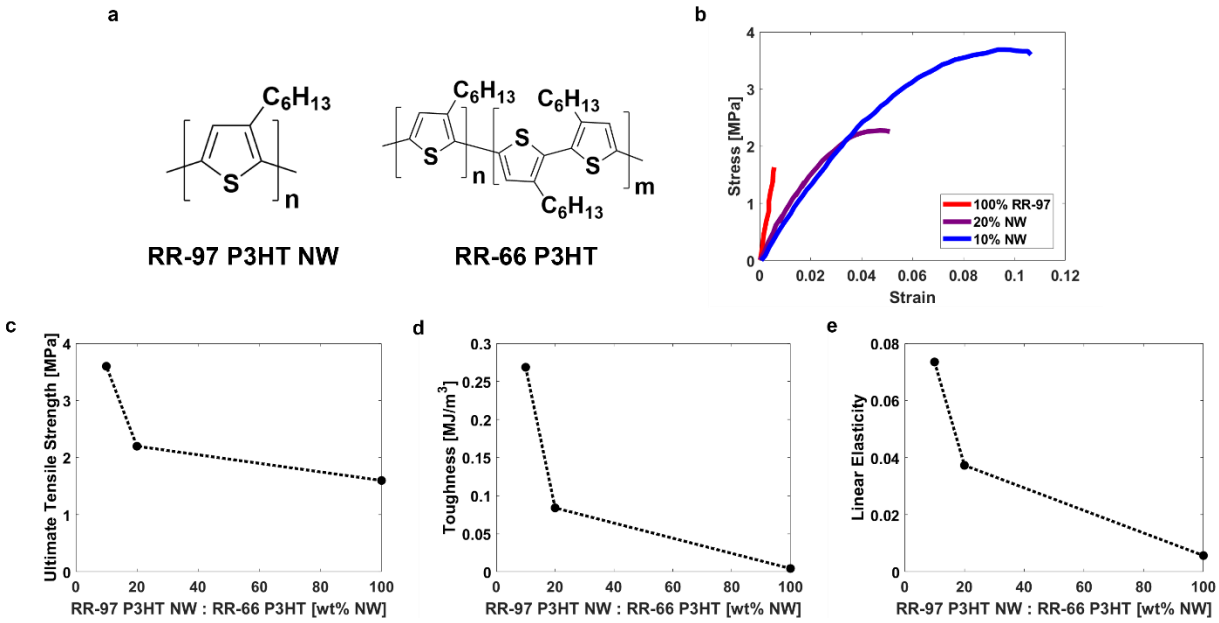

Figure S4. Mechanical properties of P3HT:NW P3HT polymer films. (a) Chemical structures of P3HT (66% regioregularity) and P3HT NWs (97% regioregularity). (b) Stress-strain curves of P3HT films as a function of nanowire loading as replotted from Kim et al. 2017.[27] Shown in red is a pure RR-97 P3HT film. (d) Tensile strength, (e) toughness, and (f) linear elasticity relative to the fraction of P3HT NWs are shown in the respective plots.

The two main differences between the samples are (1) the average regioregularity of the sample and (2) the weight fraction of highly crystalline P3HT NWs embedded in the amorphous P3HT matrix. The P3HT and P3HT NWs had similar degrees of polymerization, (97% regioregular P3HT: X_n = 111, 66% regioregular P3HT NWs X_n = 102). Likewise, their glass transition temperatures were similar (–20–0 °C).[27] As expected, the P3HT NW: P3HT blends exhibited better mechanical behavior than the pure P3HT film (which had the least favorable mechanical properties by all metrics). However, this data suggests that loading a small fraction of NWs is sufficient for improving the mechanical properties; the tensile strength, toughness, and linear elasticity were all highest for the 10% P3HT NW sample (**Fig S4c-e**).

We can infer that this improvement in mechanical properties can largely be attributed to the change in regioregularity (Main Text Section 2.2). Embedding crystalline NWs in a relatively amorphous P3HT matrix allows for increased energy dissipation by decreasing the stress concentration in the crystalline regions. This prevents early breakage of covalent bonds. As a result, the tensile strengths and fracture strains (and thus toughness) of samples with embedded NWs greatly increased (resembling that of the regioregular-*b*-regiorandom P3HT copolymers). However, we are unable to decouple the effect of the nanowires on the mechanical properties from the effect of altering the average regioregularity.

1.4 Effect of Conjugation-Break Spacers

Our main text discusses in detail the Thompson group's work studying the effects of conjugation-break spacers (CBS) on the mechanical properties of semiconducting polymers. However, two of the three libraries of polymers synthesized held the fraction of DPP and CBS units equal. This poses a problem because the mechanical effects of the DPP and CBS monomers cannot be separated from one another. The third library (a library of DPP-based polymers with a 2-ethylhexylDPP (ehDPP) monomer) attempts to isolate the effect of the CBS monomer.[29]

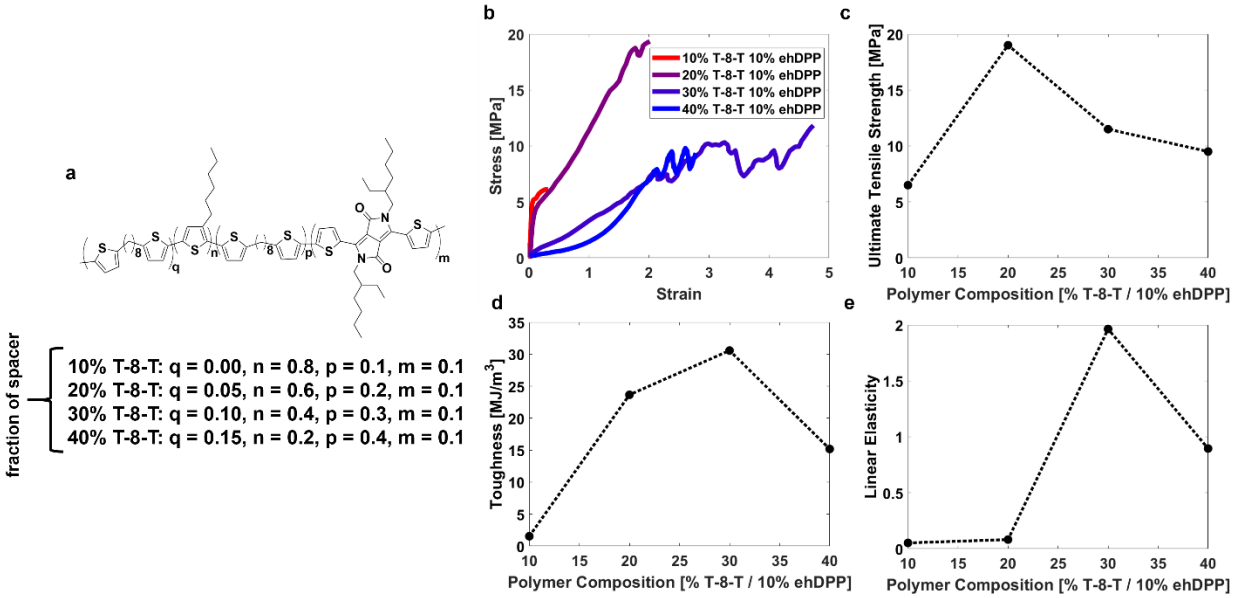

Figure S5. Mechanical properties of modified P3HT-ehDPP polymers relative to conjugation-break spacer length and fraction. (a) Chemical structure of the P3HT-ehDPP library used. Spacer fractions ranged from 10% to 40% with a constant fraction of 10% ehDPP. The spacer length likewise remained constant (alkyl length n = 8). (b) Stress-strain curves of P3HT-ehDPP polymers relative to increasing CBS fraction as reproduced from Melenbrink et al. 2019.[29] (c) Tensile strength, (d) toughness, and (e) linear elasticity are shown relative to spacer fraction.

This library of P3HT-ehDPP polymers (**Fig S5a**) holds the ehDPP monomer fraction constant at 10% while varying the fraction of the CBS unit to isolate the effect of the spacer unit. The stress-strain behaviors were difficult to interpret due to difficulties in maintaining good solubility (which creates poor quality films and thus poor mechanical measurements) and low degrees of polymerization (**Fig S5b**). The 10% CBS sample had the highest molecular weight, at 19.5 kDa, yet had the lowest tensile strength, toughness, and linear elasticity. This is in contrast to the 20% CBS sample, which had the lowest molecular weight at 8.5 kDa, but the highest tensile strength and relatively high toughness. Likewise, the 30% CBS sample had a fracture strain almost twice that of the 40% CBS sample, yet their molecular weights were relatively similar (12.8 kDa

compared to 12.4 kDa). No definitive conclusions can be drawn solely from looking at the calculated strength, toughness, and linear elasticity of these four polymers.

References

(1) Zhang, S.; Ocheje, M. U.; Luo, S.; Ehlenberg, D.; Appleby, B.; Weller, D.; Zhou, D.; Rondeau-Gagné, S.; Gu, X. Probing the Viscoelastic Property of Pseudo Free-Standing Conjugated Polymeric Thin Films. *Macromol. Rapid Commun.* **2018**, *39*, 1–8.

(2) Siviour, C. R.; Jordan, J. L. High Strain Rate Mechanics of Polymers: A Review. *J. Dyn. Behav. Mater.* **2016**, *2*, 15–32.

(3) Zhang, S.; Ocheje, M. U.; Huang, L.; Galuska, L.; Cao, Z.; Luo, S.; Cheng, Y.; Ehlenberg, D.; Goodman, R. B.; Zhou, D.; Liu, Y.; Chiu, Y.; Azoulay, J. D.; Rondeau-gagné, S.; Gu, X. The Critical Role of Electron-Donating Thiophene Groups on the Mechanical and Thermal Properties of Donor – Acceptor Semiconducting Polymers. *Adv. Electron. Mater.* **2019**, *5*, 1800898–1800899.

(4) Mulliken, A. D.; Boyce, M. C. Mechanics of the Rate-Dependent Elastic-Plastic Deformation of Glassy Polymers from Low to High Strain Rates. *Int. J. Solids Struct.* **2006**, *43*, 1331–1356.

(5) Reynolds, J. R.; Thompson, B. C.; Skotheim, T. A. *Conjugated Polymers: Properties, Processing, and Applications*; **2019**.

(6) Kraus, J.; Müller-Buschbaum, P.; Kuhlmann, T.; Schubert, D. W.; Stamm, M. Confinement Effects on the Chain Conformation in Thin Polymer Films. *Europhys. Lett.* **2000**, *49*, 210–216.

(7) Rodriquez, D.; Kim, J.; Root, S. E.; Fei, Z.; Bou, P.; Heeney, M.; Kim, T.; Lipomi, D. J.

Comparison of Methods for Determining the Mechanical Properties of Semiconducting Polymer Films for Stretchable Electronics. *ACS Appl. Mater. Interfaces* **2017**, *9*, 8855–8862.

(8) Sariban, A.; Binder, K. Critical Properties of the Flory-Huggins Lattice Model of Polymer Mixtures. *J. Chem. Phys.* **1987**, *86*, 5859–5873.

(9) Huggins, M. L. Solutions of Long Chain Compounds. *J. Chem. Phys.* **1941**, *9*, 440.

(10) Flory, P. J. Themodynamics of High Polymer Solutions. *J. Chem. Phys.* **1942**, *10*, 51–61.

(11) Wagner, H. L. The Mark-Houwink-Sakurada Equation for the Viscosity of Linear Polyethylene. *J. Phys. Chem. Ref. Data* **1985**, *14*, 611–617.

(12) Scholte, T. G.; Meijerink, N. L. J.; Schoffeleers, H. M.; Brands, A. M. G. Mark–Houwink Equation and GPC Calibration for Linear Short-chain Branched Polyolefines, Including Polypropylene and Ethylene–Propylene Copolymers. *J. Appl. Polym. Sci.* **1984**, *29*, 3763–3782.

(13) Israelachvili, J. N. *Intermolecular and Surface Forces*, 3rd ed.; 2011.

(14) Zverev, M. P.; Zubov, P. I.; Barash, A. N.; Nikonorova, L. P.; Ivanova, L. V. The Properties of Solutions of Polymers in Good and Poor Solvents and of Articles Prepared from These Solutions. *Polym. Sci. U.S.S.R.* **1974**, *16*, 589–598.

(15) Postema, A. R.; Liou, K.; Wudl, F.; Smith, P. Highly Oriented, Low-Modulus Materials from Liquid Crystalline Polymers: The Ultimate Penalty for Solubilizing Alkyl Side Chains. *Macromolecules* **1990**, *23*, 1842–1845.

(16) Lin, B.; Zhang, L.; Zhao, H.; Xu, X.; Zhou, K.; Zhang, S.; Gou, L.; Fan, B.; Zhang, L.; Yan, H.; Gu, X. D.; Ying, L.; Huang, F.; Cao, Y.; Ma, W. Molecular Packing Control Enables Excellent Performance and Mechanical Property of Blade-Cast All-Polymer Solar

Cells. *Nano Energy* **2019**, *59*, 277–284.

(17) Grell, M.; Bradley, D. D. C.; Long, X.; Chamberlain, T.; Inbasekaran, M.; Woo, E. P.; Soliman, M. Chain Geometry, Solution Aggregation and Enhanced Dichroism in the Liquid-Crystalline Conjugated Polymer Poly(9,9-Dioctylfluorene). *Acta Polym.* **1998**, *49*, 439–444.

(18) Morgan, B.; Dadmun, M. D. The Importance of Solvent Quality on the Modification of Conjugated Polymer Conformation and Thermodynamics with Illumination. *Soft Matter* **2017**, *13*, 2773–2780.

(19) Nguyen, T. Q.; Doan, V.; Schwartz, B. J. Conjugated Polymer Aggregates in Solution: Control of Interchain Interactions. *J. Chem. Phys.* **1999**, *110*, 4068–4078.

(20) Nguyen, T. Q.; Yee, R. Y.; Schwartz, B. J. Solution Processing of Conjugated Polymers: The Effects of Polymer Solubility on the Morphology and Electronic Properties of Semiconducting Polymer Films. *J. Photochem. Photobiol. A Chem.* **2001**, *144*, 21–30.

(21) Chen, J.; Zhuang, H.; Zhao, J.; Gardella, J. A. Solvent Effects on Polymer Surface Structure. *Surf. Interface Anal.* **2001**, *31*, 713–720.

(22) Schwartz, B. J. Conjugated Polymers as Molecular Materials: How Chain Conformation and Film Morphology Influence Energy Transfer and Interchain Interactions. *Annu. Rev. Phys. Chem.* **2003**, *54*, 141–172.

(23) Chang, C. C.; Pai, C. L.; Chen, W. C.; Jenekhe, S. A. Spin Coating of Conjugated Polymers for Electronic and Optoelectronic Applications. *Thin Solid Films* **2005**, *479*, 254–260.

(24) Dörling, B.; Vohra, V.; Dao, T. T.; Garriga, M.; Murata, H.; Campoy-Quiles, M. Uniaxial Macroscopic Alignment of Conjugated Polymer Systems by Directional Crystallization

during Blade Coating. *J. Mater. Chem. C* **2014**, *2*, 3303–3310.

(25) Lipomi, D. J.; Chiechi, R. C.; Dickey, M. D.; Whitesides, G. M. Fabrication of Conjugated Polymer Nanowires by Edge Lithography. *Nano Lett.* **2008**, *8*, 2100–2105.

(26) Qiu, L.; Lee, W. H.; Wang, X.; Kim, J. S.; Lim, J. A.; Kwak, D.; Lee, S.; Cho, K. Organic Thin-Film Transistors Based on Polythiophene Nanowires Embedded in Insulating Polymer. *Adv. Mater.* **2009**, *21*, 1349–1353.

(27) Kim, H. J.; Lee, M. Y.; Kim, J.; Kim, J.; Yu, H.; Yun, H.; Liao, K.; Kim, T.; Oh, J. H.; Kim, B. J. Solution-Assembled Blends of Regioregularity-Controlled Polythiophenes for Coexistence of Mechanical Resilience and Electronic Performance. *ACS Appl. Mater. Interfaces* **2017**, *9*, 14120–14128.

(28) Lu, G.; Bu, L.; Li, S.; Yang, X. Bulk Interpenetration Network of Thermoelectric Polymer in Insulating Supporting Matrix. *Adv. Mater.* **2014**, *26*, 2359–2364.

(29) Melenbrink, E. L.; Hilby, K. M.; Choudhary, K.; Samal, S.; Kazerouni, N.; McConn, J. L.; Lipomi, D. J.; Thompson, B. C. Influence of Acceptor Side-Chain Length and Conjugation-Break Spacer Content on the Mechanical and Electronic Properties of Semi-Random Polymers. *ACS Appl. Polym. Mater.* **2019**, *1*, 1107–1117.